

AN ACCURATE AND EFFICIENT PARTICLE FILTERING METHOD FOR ATTITUDE ESTIMATION USING PHOTOMETRIC MEASUREMENTS

J. Rubio^(1,2), A. de Andrés⁽¹⁾, C. Paulete⁽¹⁾, Á. Gallego⁽¹⁾, D. Escobar⁽¹⁾

⁽¹⁾ GMV, Calle Isaac Newton 11, Tres Cantos, 28670, Spain, jorge.rubio.anton@gmv.com, adandres@gmv.com, cpauleteperianez@gmv.com, agtorrego@gmv.com, descobar@gmv.com

⁽²⁾ Universidad Carlos III de Madrid, Avenida de la Universidad 30, Leganés, 28911, Spain, jorge.r.anton@alumnos.uc3m.es

ABSTRACT

The New Space era has led to an increasing congestion in Earth's orbital regions, requiring the immediate implementation of advanced Space Surveillance and Traffic (SST) methods to protect operational satellites and avoid the proliferation of space debris. Accurate knowledge of the attitude of uncontrolled space objects plays a fundamental role in this effort. This study proposes an accurate, robust and computationally efficient approach for its estimation. The method is designed to be operationally feasible and is evaluated in a realistic scenario, demonstrating excellent estimation accuracy and robustness to uncertain or unknown optical properties of space objects.

1 INTRODUCTION

The exponential increase in satellite launches into Earth's orbits over the past decade has led to a significant rise in space debris within critical orbital regions used for commercial and scientific missions. This growing congestion in space traffic requires immediate action and has become a key focus in the fields of Space Surveillance and Tracking (SST) and Space Environment Preservation (SEP).

In this context, merely estimating the orbit of inactive space objects, such as uncontrolled satellites or fragments of space debris, is no longer sufficient to ensure the safety of space operations and the long-term sustainability of the space environment. Estimating the attitude of these objects is crucial for many applications, including improving collision risk assessments and atmospheric re-entry predictions, designing Active Debris Removal (ADR) and In-Orbit Servicing (IOS) missions, and detecting anomalies in both active and inactive satellites. The attitude of space objects can be estimated from light curves, namely, the temporal variation of sunlight reflected by these objects and detected by ground-based optical sensors.

Previous efforts to estimate the attitude of space objects from light curves have employed techniques such as the Unscented Kalman Filter (UKF), either assuming precise knowledge of an object's geometric and optical properties [1,2] or attempting to estimate its shape simultaneously

with its rotational and translational states using a Multiple-Model Adaptive Estimation (MMAE) approach [3]. A common conclusion of these analyses is the presence of measurement ambiguities, that is, the existence of multiple attitude states or combinations of attitude states and object physical properties that produce very similar light curves.

The potential existence of multiple solutions, combined with the highly non-linear measurement function, may result in a non-Gaussian and multimodal posterior probability distribution. Therefore, Bayesian sequential estimation methods have also been explored as an alternative to the UKF. The Sample Importance Resampling (SIR) particle filter has been used in different studies to estimate the attitude, assuming known geometric properties [4], and also addressing shape model uncertainty and tracking actively manoeuvring satellites [5]. Other variants of the particle filter have also been investigated, such as the Rao-Blackwellised Particle Filter (RBPF) to improve computational performance [6], the Unscented Particle Filter (UPF) [7], or a combination of two SIR particle filters to improve estimation accuracy [8].

Other methods that have been investigated consist of a combination of different techniques, such as the Adaptive Gaussian Mixtures Unscented Kalman Filter (AGMUKF) proposed in [9], where the UKF is used to propagate and update the kernels of the Gaussian mixture employed to estimate the probability density function, and the use of Gaussian Process Regression (GPR) in [10] to build a non-parametric observation model that is combined with the UKF. Optimisation algorithms have also been explored, particularly Particle Swarm Optimisation (PSO). It has been used to estimate attitude, shape and optical properties simultaneously [11], or to model arbitrary torque-free attitude motion, assuming that the object's shape and reflective properties are known in a two-step estimation technique [12].

This work focuses on the estimation of the attitude of uncontrolled space objects with known geometric properties at a specific time. The objective is analogous to that of Initial Orbit Determination (IOD), where orbital parameters are estimated with no a priori knowledge, typically at the time of the most recent sensor

measurement. The primary goal of the proposed approach is to provide an accurate, robust and computationally efficient solution that can be applied in real operational scenarios. The worst-case scenario, where only measurements from a single sensor are available, is considered. Examples of operational use cases for this approach include the design of debris mitigation missions, such as Active Debris Removal (ADR) and In-Orbit Servicing (IOS), as well as the monitoring of active satellites to detect anomalies.

2 METHODS

This section introduces a novel approach for estimating attitude from light curves in operational scenarios. As explained in Section 1, estimation methods that require a precise initial guess, such as the UKF, often struggle to find the correct solution. This is due to measurement ambiguities that can cause these methods to become trapped in local optima. While particle filters can overcome this limitation, they operate sequentially, making them less suitable for this specific application. In operational scenarios, photometric measurements are only available during the object's visibility interval, and the complete light curve is typically processed after the observation period has ended.

Consequently, the proposed attitude estimation method efficiently explores the entire solution space without relying on an initial guess. Additionally, photometric measurements are processed using a batch strategy, focusing on estimating the attitude at a specific time rather than tracking its evolution over the visibility interval. This approach mitigates measurement ambiguities and allows the parallelisation of computations to improve the method's efficiency.

To achieve these objectives, the proposed approach integrates statistical techniques—Adaptive Importance Sampling and Systematic Resampling—with a population-based optimisation method, Particle Swarm Optimisation. The fundamentals of these methods and their integration are explained in Section 2.3. Before this, the attitude and observation models used to propagate the attitude state and simulate photometric measurements are described in Sections 2.1 and 2.2, respectively.

2.1 Attitude model

The evolution of the attitude state over the visibility interval can be accurately modelled kinematically, as the effects of perturbing torques from forces such as non-uniform gravitational fields, eddy currents, solar radiation pressure and atmospheric drag are negligible over the short duration of the visibility interval. In fact, considering the dynamics would not significantly improve the estimation in a real-world scenario, as important parameters such as the eddy currents tensor and mass distribution are typically unknown.

The kinematic evolution of the attitude during a single pass over the sensor can be modelled as a purely spinning motion, in which the object rotates around a fixed axis with a constant angular velocity. This assumption is realistic, as energy dissipation causes space objects that have not undergone collisions or explosions for a long time to adopt a flat spin. In this state, they rotate around their principal axis of maximum inertia, which remains stable in free space [13]. Even if the object exhibits precession, its precession period is typically longer than the duration of the visibility interval [14], meaning that the sensor perceives only a spinning motion.

Considering a body-fixed reference frame B , attached to the space object, and an inertial reference frame I , such as the Geocentric Celestial Reference Frame (GCRF), the general kinematic equation governing the rotational motion of a rigid body is [15]:

$$\dot{\mathbf{q}}_B^I = \frac{1}{2} \mathbf{q}_B^I \otimes \boldsymbol{\omega}_{q,B/I} = \frac{1}{2} \boldsymbol{\Omega} \mathbf{q}_B^I \quad (1)$$

$$\boldsymbol{\Omega} = \boldsymbol{\Omega}(\boldsymbol{\omega}_{q,B/I}) = \begin{bmatrix} 0 & -\omega_x & -\omega_y & -\omega_z \\ \omega_x & 0 & \omega_z & -\omega_y \\ \omega_y & -\omega_z & 0 & \omega_x \\ \omega_z & \omega_y & -\omega_x & 0 \end{bmatrix} \quad (2)$$

where \mathbf{q}_B^I is the quaternion representing the rotation of frame B relative to frame I at some time t , and $\boldsymbol{\omega}_{q,B/I} = [0, \boldsymbol{\omega}_{B/I}]^T = [0, \omega_x, \omega_y, \omega_z]^T$ is the quaternion representation of the instantaneous angular velocity of frame B relative to frame I , expressed in the rotating frame B .

Since the components of the angular velocity are assumed to be constant, the matrix $\boldsymbol{\Omega}$ is constant and Eq. (3) can be readily integrated to obtain the following closed-form solution for the kinematic equation:

$$\begin{aligned} \mathbf{q}_B^I(t) &= \exp\left(\frac{1}{2} \boldsymbol{\Omega} t\right) \mathbf{q}_{B,0}^I \\ &= \left[\cos\left(\frac{\omega_{B/I}}{2} t\right) \mathbf{I} + \frac{1}{\omega_{B/I}} \sin\left(\frac{\omega_{B/I}}{2} t\right) \boldsymbol{\Omega} \right] \mathbf{q}_{B,0}^I \end{aligned} \quad (3)$$

where $\mathbf{q}_{B,0}^I$ is the quaternion representing the reference attitude state that the proposed estimation method aims to determine using photometric measurements.

2.2 Observation model

The observation model used in this work is based on the bidirectional reflectance distribution function (BRDF), which determines how sunlight is reflected from the surfaces of the space object. Since ambient illumination in outer space is negligible, the BRDF can be readily decomposed into diffuse and specular components.

The specular component models highlights, i.e. light reflected directly from the material's surface along the mirror direction. The Cook-Torrance specular BRDF [16] is used, with the Fresnel factor computed according to Schlick's model [17]. For the facet slope distribution function, the Beckmann distribution originally proposed by Cook and Torrance is replaced with the GGX model introduced by Walter et al. [18]. On the other hand, the diffuse component represents light scattered approximately equally in all directions, and the Lommel-Seeliger diffuse BRDF [19] is used in this work.

Once the incident irradiance detected by the sensor I_o is determined, the apparent magnitude of the space object can be computed as:

$$m = -2.5 \log \left(\frac{I_o}{I_{ref}} \right) + T(\lambda, h, \theta, aod_{550}) \quad (4)$$

where $I_{ref} = 2.518 \times 10^{-8} \text{ W/m}^2$ corresponds to the zero point of the apparent bolometric magnitude scale. The atmospheric light extinction model proposed in [20] is considered with a transmission factor $T(\lambda, h, \theta, aod_{550})$ that depends on the mean wavelength of light λ , the observer's altitude above mean sea level h , the elevation angle of the observed space object relative to the ground station θ , and the optical depth of atmospheric aerosols at a wavelength of 550 nm aod_{550} .

This observation model is implemented in **Grial**, GMV's high-fidelity light curve simulator, which allows to model the actual optical properties of each surface of the space object and considers self-shadowing interactions between different parts of the object. **Grial** uses OpenGL to graphically compute the contribution of each illuminated and visible surface pixel to the reflected light, achieving an average simulation performance of 1.4 ms per observation.

2.3 Attitude estimation method

This section introduces the proposed attitude estimation method based on light curves, specifically designed for scenarios where no prior knowledge of the attitude is available. To mitigate measurement ambiguities and improve computational efficiency, photometric measurements are processed using a batch strategy. The methodology is developed with an operational focus, prioritising accuracy and rapid convergence to the correct solution while ensuring robustness to uncertain or unknown optical properties of the space object.

To achieve these objectives, the proposed attitude estimation method integrates Adaptive Importance Sampling, Systematic Resampling and Particle Swarm Optimisation. The algorithm of the complete attitude estimation approach is presented in Figure 2-1 followed by an explanation of the fundamentals of each method and the details of their integration.

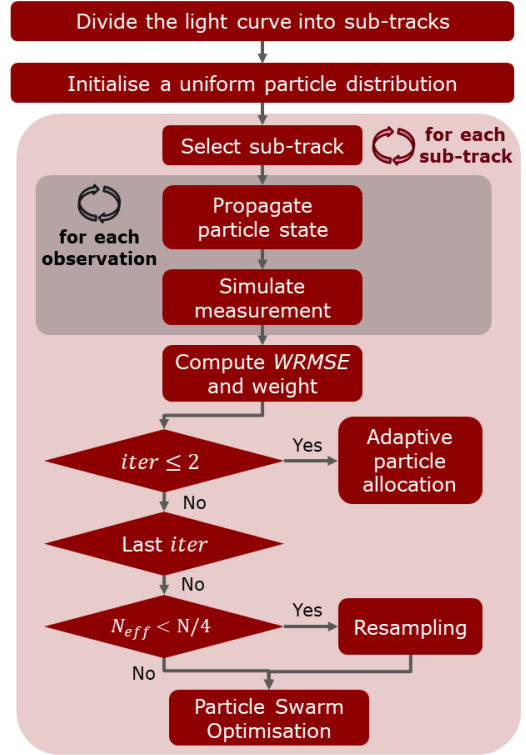


Figure 2-1. Attitude estimation algorithm

Considering a vector \mathbf{x} of unknown attitude parameters with a probability density function $\pi(\mathbf{x})$, Adaptive Importance Sampling (AIS) [21] approximates the unknown target probability density function by drawing samples from a proposal distribution $q(\mathbf{x})$. Each sample is assigned an importance weight that quantifies its contribution to the approximation of the target distribution. In the context of Bayesian inference, the importance weight function is given by

$$w(\mathbf{x}) = \frac{\pi(\mathbf{x})}{q(\mathbf{x})} = \frac{\ell(\mathbf{z}|\mathbf{x})p_0(\mathbf{x})}{q(\mathbf{x})} \quad (5)$$

where \mathbf{z} is a vector of observed data, and the target distribution $\pi(\mathbf{x})$ is expressed in terms of the likelihood function $\ell(\mathbf{z}|\mathbf{x})$, and the prior probability density function $p_0(\mathbf{x})$ in accordance with Bayes' theorem.

AIS methods are iterative and consist of three fundamental steps: sampling from the proposal densities, computing the importance weights of each sample, and updating the proposal densities for the subsequent iteration. As previously mentioned, batch processing of photometric measurements is used to mitigate the effects of measurement ambiguity. Therefore, the light curve is divided into sub-tracks using the inertial rotation period as the sampling step. In each iteration of the AIS method, one sub-track is processed, incorporating all its photometric measurements to compute the importance weights.

The weighted root mean squared error (*WRMSE*) is selected as one of the particle quality metrics, as it is well-suited for handling measurements from multiple sensors with different noise levels:

$$WRMSE = \sqrt{\frac{1}{K} \sum_{j=1}^K \left(\frac{y_j - z_j}{\sigma_{s,j}} \right)^2} \quad (6)$$

where z_j is a real photometric observation, y_j is a simulated measurement corresponding to a given particle state at the time of the real measurement z_j , and $\sigma_{s,j}$ denotes the sensor noise standard deviation associated with the real measurement z_j .

The normalised particle weights are computed using Eq. (7), obtained from Eq. (5) by setting the importance density equal to the prior density at each iteration of the AIS method, i.e. $q(\mathbf{x}) = p_0(\mathbf{x})$:

$$\begin{aligned} \bar{w}_i &= \ell \left(\{z_j\}_{j=1}^K \mid \mathbf{x}_i \right) \\ &= \frac{\exp(-WRMSE_i^2)}{\sum_{i=1}^N \exp(-WRMSE_i^2)} \end{aligned} \quad (7)$$

where the likelihood function represents the probability of observing a set of photometric measurements given the particle state. As shown in Eq. (7), the particle *WRMSE* is mapped to a probability using a softmax function.

Before describing the update step of the AIS method, it is important to note that during the first two iterations, an adaptive allocation of particles is performed to refine the initial proposal distribution. This process consists of relocating particles from low-probability density regions to areas of higher probability density. Specifically, particles with a *WRMSE* exceeding 110 % of the average *WRMSE* of the existing particles are moved towards those with the lowest *WRMSE*. The new positions of these particles are determined based on the sampling step of the initial distribution, ensuring that they are placed at intermediate positions between the existing ones.

Finally, the update step is carried out by integrating Systematic Resampling and Particle Swarm Optimisation to improve computational efficiency. Systematic Resampling [22] is used to prevent particle degeneracy, a phenomenon in which a small number of particles have significant weight while the majority contribute minimally to the overall estimate. This resampling step is performed if the effective sample size, given by Eq. (8), falls below 25 % of the total number of particles.

$$N_{eff} = \frac{1}{\sum_{i=1}^N \bar{w}_i^2} \quad (8)$$

Particle Swarm Optimisation (PSO) [23] is a population-based global optimisation algorithm used in this case to estimate the target distribution implicitly, thereby avoiding the computational cost of explicitly computing it at each iteration. Additionally, PSO offers a more efficient alternative to conventional methods used in particle filters to enhance particle diversity, such as the introduction of artificial noise, enabling faster convergence to the correct attitude solutions.

In PSO, particles move through the search space based on their momentum. The velocity of the particles is computed at each iteration k to update their trajectory according to the following expressions:

$$\begin{aligned} \mathbf{v}_k^i &= w\mathbf{v}_{k-1}^i + c_1 r_1 (\mathbf{x}_{pbest}^i - \mathbf{x}_k^i) \\ &\quad + c_2 r_2 (\mathbf{x}_{gbest} - \mathbf{x}_k^i) \\ \mathbf{x}_k^i &= \mathbf{x}_{k-1}^i + \mathbf{v}_k^i \end{aligned} \quad (9)$$

where w is the inertia weight factor, c_1 is the cognitive coefficient, \mathbf{x}_{pbest}^i is the best position found by the particle (personal best), c_2 is the social coefficient, \mathbf{x}_{gbest} is the best position found by any particle in the swarm (global best), and r_1 and r_2 are random numbers drawn from $U(0,1)$.

In the attitude estimation method proposed in this work, the solution space is initially explored through the adaptive allocation of particles during the first iterations. Therefore, the PSO coefficients are primarily chosen to accelerate convergence towards optimal solutions. To promote local exploration in the early stages of optimisation while gradually shifting towards exploitation by guiding particles to global best states, the cognitive coefficient is decreased linearly, while the social coefficient is increased linearly as iterations progress [24]:

$$\begin{aligned} c_1(k) &= c_{1,max} + \frac{k}{K} (c_{1,min} - c_{1,max}) \\ c_2(k) &= c_{2,min} + \frac{k}{K} (c_{2,max} - c_{2,min}) \end{aligned} \quad (10)$$

where the social coefficient is consistently set higher than the cognitive coefficient across all iterations by selecting $c_{1,min} = 0.5$, $c_{1,max} = 1.5$, $c_{2,min} = 1.0$, $c_{2,max} = 2.0$, and $K = 3$. Once the iteration count of the PSO exceeds K , the values of c_1 and c_2 remain fixed at their values from iteration K for all subsequent iterations. The inertia weight factor remains constant throughout all iterations, with a value of $w = 0.3$.

The attitude estimation problem using light curves is strongly influenced by the coupling between attitude, geometric properties and surface optical characteristics. This coupling implies that different combinations of these parameters can produce nearly identical light

curves. The proposed method is designed to be robust against uncertainties in the object's surface optical properties, which are inherently difficult to determine due to the wide variety of materials and their degradation from prolonged exposure to the space environment [RD.43].

A potential strategy to improve the method's robustness against uncertain or unknown optical properties could involve estimating the reflective characteristics of each surface. However, the proposed approach is constrained by the curse of dimensionality, and increasing the problem's dimensionality results in unacceptable computational performance in operational scenarios. To address this challenge, this work presents an accurate and robust alternative that preserves computational efficiency.

The study by Qiao et al. [25] demonstrated that the primary factor influencing the reflectance spectra of three-axis stabilised GEO satellites is the presence of multi-layer insulation (MLI) on the platform's surface. Rodriguez et al. [26] analysed various types of MLI materials and reported significant variability in their reflectance, ranging from 0.05 to 0.25. Due to the irregularities of MLI on satellite surfaces, it can be modelled as a purely diffuse reflector. Similarly, Mulrooney et al. [27] recommended using a global albedo of 0.175 for debris objects, although the later work by Mulrooney et al. [28] reported variability in this reference value, ranging from 0.12 to 0.275. Regarding solar arrays, they can be considered predominantly specular reflectors. The studies by Hall [29] and Cao et al. [30] suggest that solar arrays reflect with an albedo of approximately 0.1, with minimal dispersion.

In light of these previous studies, the proposed attitude estimation method aims to incorporate a global diffuse coefficient for the platform or main body of the space object to accurately estimate its attitude state. Two approaches will be examined: one in which a fixed global diffuse coefficient is predefined, and another where the global diffuse coefficient is estimated alongside the attitude of the space object. As suggested by previous studies in the literature, the solar arrays are modelled as purely specular reflectors with a specular reflection coefficient of $k_s = 0.1$.

3 RESULTS

This section presents the results of the analyses conducted to evaluate the proposed attitude estimation method. The study considers a satellite in a circular orbit at an altitude of 2000 km. The satellite model used in the simulations, depicted in Figure 3-1, consists of a quadrangular prism platform with dimensions of $2.5 \times 1 \times 1$ m and a solar array measuring $1.5 \times 3.5 \times 0.01$ m, resulting in a total span of 9 m.

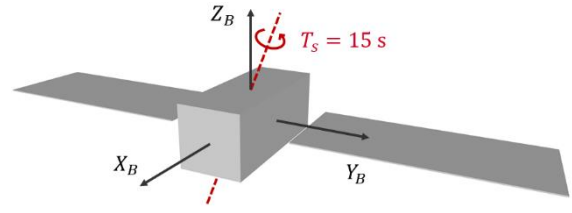


Figure 3-1. Satellite model

The reference light curve is presented in Figure 3-2. This light curve has been generated based on the following reference orientation, expressed in terms of Euler angles—yaw, pitch and roll—which represents the satellite orientation that must be estimated from the light curve:

$$\mathbf{x}_{ref} = [71, -58, 19]^T \text{ deg}$$

Both the spin period and axis are assumed to be known, as they can be estimated using alternative methods [29]. Specifically, the spin period is set to 15 s and a 7 deg deviation from the satellite's Z_B axis is considered for the spin axis. This scenario is representative of a satellite that has not experienced explosions or collisions for a long time and eventually adopts a flat spin around its principal axis of maximum inertia.

In addition, the reference light curve is generated by modelling all platform surfaces with a diffuse reflection coefficient of $k_d = 0.15$, and the solar arrays as purely specular reflectors with a specular coefficient of $k_s = 0.1$. The reference light curve has been simulated assuming a sensor noise level of $\sigma_s = 0.1$ in magnitude.

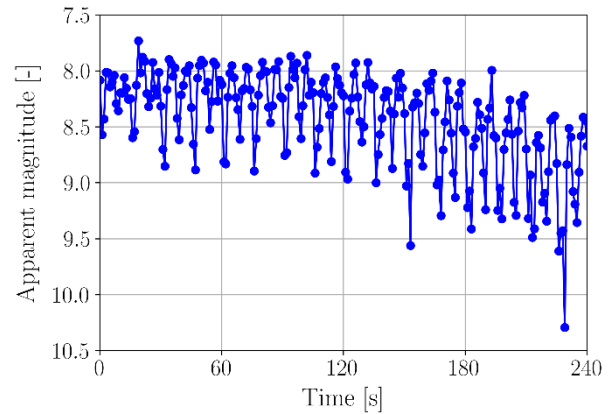


Figure 3-2. Reference light curve

The execution of the attitude estimation method assuming both known geometric and optical properties is described below. Figure 3-3 shows the distribution of particles across different iterations of the method. In all plots, the actual attitude state to be estimated is indicated by a red cross. The numerical results of the estimation method at the last iteration are presented in Table 3-1, including the weighted attitude state and the weighted standard deviation.

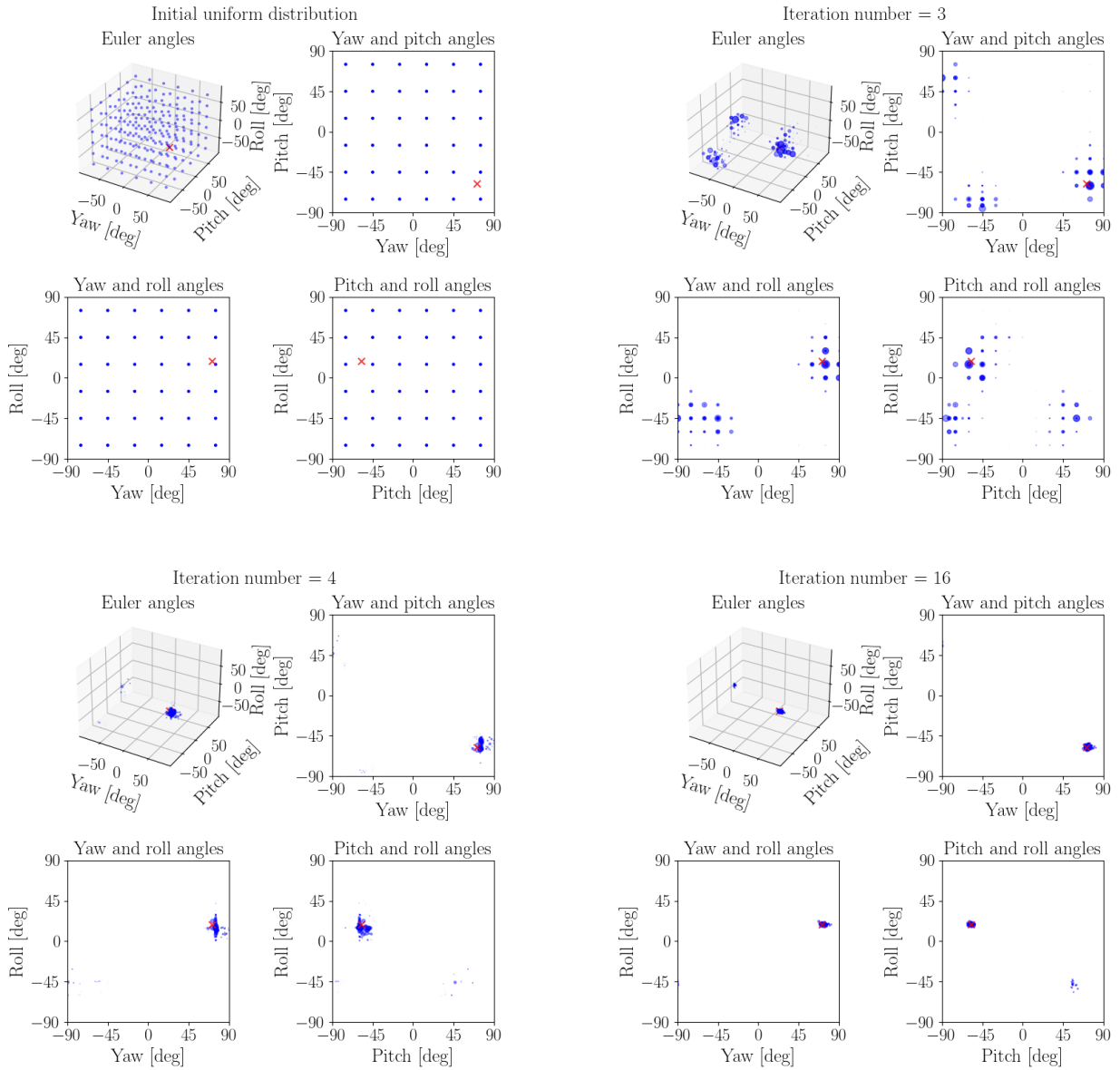


Figure 3-3. Execution of the attitude estimation method with known optical properties

Firstly, the light curve is divided into sub-tracks based on the inertial rotation period of 15 s and the total observation interval of 4 min, resulting in 16 sub-tracks. Then, a uniform distribution of particles is generated across the solution space, constrained by the symmetric geometric and optical properties of the satellite model. A sampling step of 30 deg is selected for each angular state parameter, obtaining 216 particles, thereby ensuring a sufficiently fine grid for accurate attitude estimation. The execution of all 16 iterations is completed in 30 seconds, although the process could be terminated much earlier, as convergence is achieved by the sixth iteration.

The first two iterations of the attitude estimation method focus on exploring the search space through the adaptive allocation of particles, ensuring that all promising candidate solutions are identified. By the third iteration, three higher-probability density regions are identified, after which the combined effects of Systematic Resampling and PSO further refine these candidate solutions. By the final iteration, all particles have converged around the true attitude state. The *WRMSE* between the light curve simulated using the estimated attitude and the reference light curve is 0.1213, which closely aligns with the sensor noise standard deviation.

Table 3-1. Results of the attitude estimation method for an object with known optical properties

	Reference	Result
Yaw [deg]	71	72.79 ± 0.12
Pitch [deg]	-58	-57.59 ± 0.10
Roll [deg]	19	18.72 ± 0.06

The next step of the analysis aims to assess the robustness of the proposed method to uncertainties in the optical properties of the space object. As explained in Section 2.3, the solar arrays are well characterised by a purely specular behaviour with $k_s = 0.1$, and therefore, they are not considered in this analysis. The focus of the study is on the platform, as its surfaces may consist of various components and/or materials, each with a wide range of diffuse reflection coefficients. Consequently, the analysis focuses on varying the diffuse coefficient of one of the surfaces that has the greatest impact on many of the photometric measurements in the light curve. The attitude is then estimated using a single global diffuse coefficient for all surfaces of the object.

The first study evaluates the robustness of the method assuming a typical value for the global diffuse coefficient. To this end, the reference light curve is generated by changing the diffuse reflection coefficient of one of the surfaces with the greatest impact on the light curve to $k_d = 0.3$. Its symmetric surface is also modified to maintain the symmetry of the model, while the remaining surfaces retain a $k_d = 0.15$. The attitude is then estimated using a fixed global diffuse coefficient, in this case $k_{d,global} = 0.15$, which approximates the reflective behaviour of the MLI.

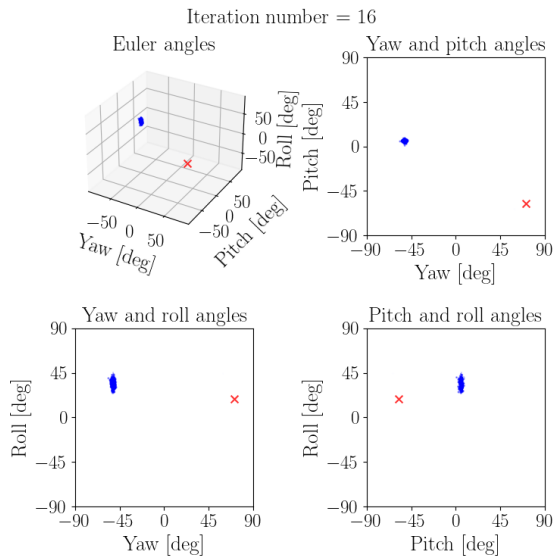


Figure 3-4. Robustness analysis using a fixed $k_{d,global}$

The results of the attitude estimation method at the last iteration are shown in Figure 3-4, where it is clear that the method converges to an attitude that does not correspond to the actual one. The number of particles has been increased to 729 (using an initial sampling step of 20 deg) to ensure that the result of the analysis is independent of the number of particles.

To make the method robust to uncertain or unknown optical properties of the space object, the attitude estimation method is extended to also estimate a global diffuse coefficient for the satellite platform. This global diffuse coefficient is expected to represent an average of the different diffuse reflection coefficients of the surfaces, weighted according to the relative impact each surface has on the resultant light curve.

Two test cases are considered in this robustness analysis. The diffuse reflection properties used to generate the reference light curve for each test case are provided in Table 3-2. Since there are four faces of equal dimensions (the lateral faces of the quadrangular prism), the change in k_d is applied to the surfaces whose normal is aligned with the $\pm Y_B$ direction. This approach ensures a reliable assessment, as the surfaces aligned with the $\pm X_B$ and $\pm Y_B$ directions—now exhibiting different k_d values—, have approximately the same relative influence on the resulting light curve.

Table 3-2. Diffuse reflection coefficient of the satellite platform's surfaces for the robustness analyses

	k_d [-]	
	Test case 1	Test case 2
Surfaces $\pm X_B$	0.15	0.15
Surfaces $\pm Y_B$	0.30	0.60
Surfaces $\pm Z_B$	0.15	0.15

Figure 3-5 and Figure 3-6 present the results of the robustness analysis for Test case 1 and Test case 2, respectively. Specifically, these figures show the estimated attitude and global diffuse reflection coefficient at the final iteration of the proposed attitude estimation method. The numerical results of the robustness analyses are presented in Table 3-3, including the weighted attitude state, its associated weighted standard deviation, and the weighted global diffuse coefficient at the final iteration of the attitude estimation method. As it can be observed, the estimated global diffuse reflection coefficient closely approximates the average k_d of the satellite platform's surfaces used to generate the reference light curve. Notably, the estimation accuracy improves as the discrepancy in k_d

between different surfaces decreases. Nevertheless, even in the more challenging Test Case 2, the results remain highly accurate.

When the method was constrained to a fixed global diffuse reflection coefficient, convergence to the correct solution was not achieved. In contrast, allowing the method to estimate this parameter provides successful convergence to the correct attitude, even in the more challenging Test case 2. This case represents an extreme scenario in which some surfaces exhibit very low k_d values, such as those characteristic of MLI, while others have significantly higher values, such as those typical of white paint [32] or some aluminium alloys [33,34].

Table 3-3. Results of the attitude estimation method for an object with unknown optical properties

	Ref.	Test case 1	Test case 2
Yaw [deg]	71	69.83 ± 0.03	74.57 ± 0.02
Pitch [deg]	-58	-60.33 ± 0.03	-62.30 ± 0.03
Roll [deg]	19	19.21 ± 0.04	14.33 ± 0.02
$k_{d,global}$ [-]	-	0.243	0.369

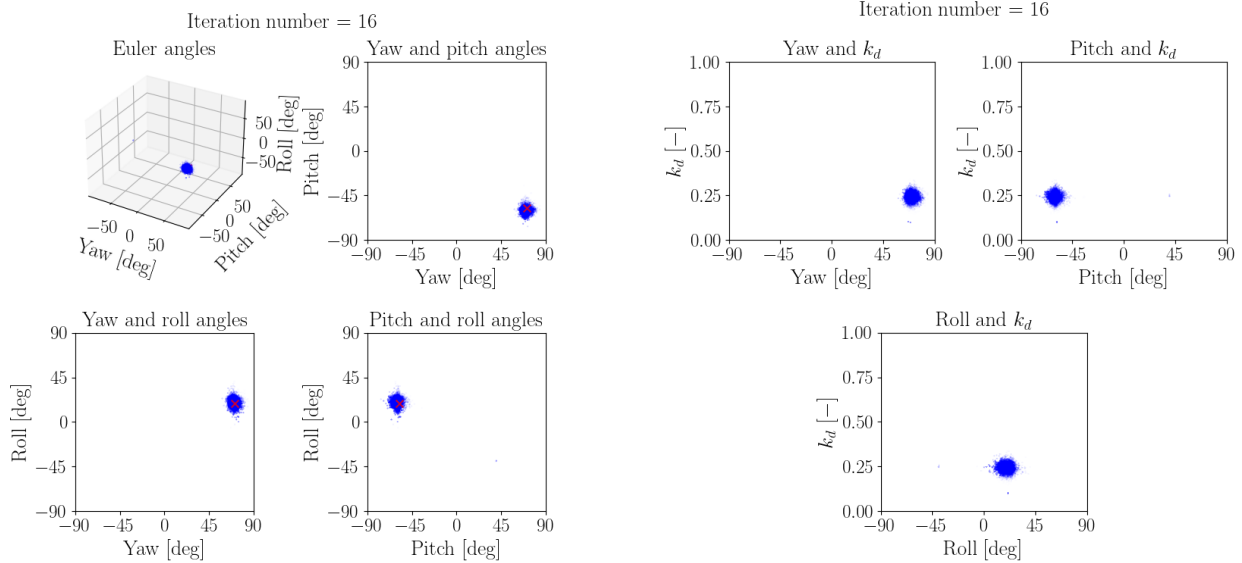


Figure 3-5. Result of the robustness analysis for Test case 1

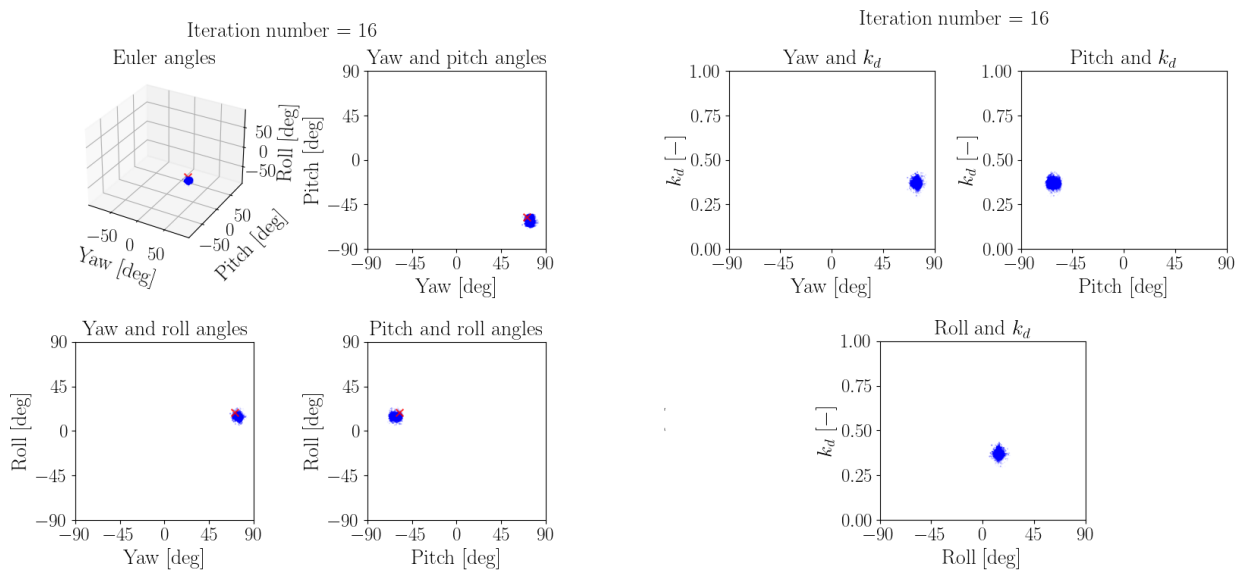


Figure 3-6. Result of the robustness analysis for Test case 2

4 CONCLUSIONS

A novel attitude estimation method using light curves has been proposed. The methodology is designed with an operational focus to ensure accuracy, robustness and computational efficiency. To that end, it integrates statistical techniques —Adaptive Importance Sampling (AIS) and Systematic Resampling— with a population-based optimisation method, Particle Swarm Optimisation (PSO). This hybrid solution effectively leverages the strengths of each method while mitigating their respective limitations, resulting in a highly efficient and reliable attitude estimation method.

The proposed approach is also demonstrated to be robust against unknown optical properties of a space object's surfaces. This is crucial for real operations, as the diverse range of aerospace materials makes precise characterisation challenging. Moreover, even when the material properties are initially known, prolonged exposure to the space environment can significantly alter them over time. The results of the test cases show exceptional accuracy in attitude estimation, even in the most challenging scenario involving surfaces with significantly different diffuse reflection coefficients. This demonstrates the method's reliability and its strong potential for real SST operations.

Possible lines of future work include implementing a clustering algorithm to assess particle convergence and terminate the execution of the attitude estimation method accordingly. Moreover, techniques to refine the estimation will be explored. Possible approaches include re-executing the proposed estimation method — potentially incorporating the estimation of each space object's optical properties— or employing the Unscented Kalman Filter, which offers greater computational efficiency for this purpose. The analysis could also be extended to account for an unknown spin axis and period. In particular, estimating the inertial rotation period from the apparent one would be especially valuable, as the latter can be directly inferred from the light curve using methods such as the Lomb-Scargle periodogram. Finally, strategies to improve the method's robustness against uncertain atmospheric conditions, particularly the aerosol optical depth (AOD), will also be investigated.

ACKNOWLEDGEMENTS

The authors express their gratitude to Prof. Joaquín Míguez from Universidad Carlos III de Madrid for introducing them to Adaptive Importance Sampling methods and providing invaluable insights on their application.

This project has received funding from the “Comunidad de Madrid” under the “Ayudas destinadas a la realización de doctorados industriales” program (project IND2023/TIC-28739).

REFERENCES

1. Wetterer, C.J. & Jah, M. (2009). Attitude Determination from Light Curves. *Journal of Guidance, Control, and Dynamics* 32(5), 1648-1651.
2. Bernard, A.J. (2021). *Attitude and Reflection Parameter Estimation of Resident Space Objects Using Ground-Based Photometry*. All Graduate Theses and Dissertations, Spring 1920 to Summer 2023, No. 8187.
3. Linares, R., Crassidis, J., Jah, M. & Kim, H. (2010). Astrometric and Photometric Data Fusion for Resident Space Object Orbit, Attitude, and Shape Determination Via Multiple-Model Adaptive Estimation. In *AIAA Guidance, Navigation, and Control Conference*, August 2010.
4. Linares, R., Crassidis, J. & Jah, M. (2014). Particle Filtering Light Curve Based Attitude Estimation for Non-Resolved Space Objects. *Advances in the Astronautical Sciences* 152, 119-130.
5. Holzinger, M.J., Alfried, K. T., Wetterer, C.J., Luu, K.K., Sabol, C. & Hamada, K. (2014). Photometric Attitude Estimation for Agile Space Objects with Shape Uncertainty. *Journal of Guidance, Control, and Dynamics* 37(3), 921-932.
6. Coder, R.D., Holzinger, M.J. & Linares, R. (2018). Three-Degree-of-Freedom Estimation of Agile Space Objects Using Marginalized Particle Filters. *Journal of Guidance, Control, and Dynamics* 41(2), 388-400.
7. Du, X., Wang, Y., Hu, H., Gou, R. & Liu, H. (2018). The Attitude Inversion Method of Geostationary Satellites Based on Unscented Particle Filter. *Advances in Space Research* 61(8), 1984-1996.
8. Wang, Y., Du, X., Gou, R., Liu, Z. & Chen, H. (2023). A Secondary Particle Filter Photometric Data Inversion Method of Space Object Characteristics. *Electronics* 12(9), Article 2044.
9. Cabrera, D.V., Utzmann, J. & Förstner, R. (2023). The Adaptive Gaussian Mixtures Unscented Kalman Filter for Attitude Determination Using Light Curves. *Advances in Space Research* 71(6), 2609-2628.
10. Hara, R., Yoshimura, Y. & Hanada, T. (2024). Photometric Attitude Estimation Using Gaussian Process Regression. In *Advanced Maui Optical and Space Surveillance (AMOS) Technologies Conference*, September 2024, pp. 96.

11. Clark, R., Dave, S., Wawrow, J. & others (2020). Performance of Parameterization Algorithms for Resident Space Object (RSO) Attitude Estimates. In *Proceedings of the Advanced Maui Optical and Space Surveillance Technologies*, Maui, HI, USA, 2020, pp. 15-18.
12. Burton, A., Robinson, L. & Frueh, C. (2024). Light Curve Attitude Estimation Using Particle Swarm Optimizers. *Advances in Space Research* 74(11), 5619-5638.
13. Schaub, H. & Junkins, J.L. (2009). *Analytical Mechanics of Space Systems* (2nd ed.). AIAA Education Series, Reston, VA.
14. Fu, X.J., Wang, M., Wang, C. & Gao, M.G. (2010). Attitude Stability Determination Based on RCS Series Information Extraction for Space Objects. In *Information Technology for Manufacturing Systems, Applied Mechanics and Materials*, Vol. 20, Trans Tech Publications Ltd, pp. 936-941.
15. Wertz, J.R. (1978). Attitude Prediction. In *Spacecraft Attitude Determination and Control* (J.R. Wertz, Ed.), Springer Netherlands, Dordrecht, pp. 558-587.
16. Cook, R.L. & Torrance, K.E. (1982). A Reflectance Model for Computer Graphics. *ACM Trans. Graph.* 1(1), 7–24. Association for Computing Machinery, New York, NY, USA.
17. Schlick, C.M. (1994). An Inexpensive BRDF Model for Physically-based Rendering. *Computer Graphics Forum* 13.
18. Walter, B., Marschner, S.R., Li, H. & Torrance, K.E. (2007). Microfacet Models for Refraction Through Rough Surfaces. In *Proc. 18th Eurographics Conference on Rendering Techniques*, Eurographics Association, Goslar, DEU, pp. 195–206.
19. Fairbairn, M.B. (2005). Planetary Photometry: The Lommel-Seeliger Law. *Journal of the Royal Astronomical Society of Canada*, 99(3), 92–93.
20. Buil, C. (2009). Le calcul de la transmission spectrale atmosphérique: application à la surveillance de l'activité de d'étoiles faibles. <http://www.astrosurf.com/aras/extinction/calcul.htm> (accessed 19 December 2024).
21. Bugallo, M.F., Elvira, V., Martino, L., Luengo, D., Míguez, J. & Djuric, P.M. (2017). Adaptive Importance Sampling: The Past, the Present, and the Future. *IEEE Signal Processing Magazine* 34(4), 60–79.
22. Kitagawa, G. (1996). Monte Carlo Filter and Smoother for Non-Gaussian Nonlinear State Space Models. *Journal of Computational and Graphical Statistics*, 5(1), 1-25.
23. Kennedy, J. & Eberhart, R. (1995). Particle Swarm Optimization. In *Proceeding of ICNN'95 - International Conference on Neural Networks*, 4, 1942-1948.
24. Ratnaweera, A., Halgamuge, S.K. & Watson, H.C. (2004). Self-Organizing Hierarchical Particle Swarm Optimizer With Time-Varying Acceleration Coefficients. *IEEE Transactions on Evolutionary Computation*, 8(3), 240-255.
25. Qiao, Q., Ping, Y., Chen, J., Lu, Y., & Zhang, C. (2024). Investigation of factors affecting the reflectance spectra of GEO Satellites. *Advances in Space Research* 74(7), 3028-3044.
26. Rodriguez, H., Abercromby, K., Mulrooney, M. & Barker, E. (2007). Optical Properties of Multi-Layered Insulation. In *Proceedings of the 2007 AMOS Conference*.
27. Mulrooney, M., Matney, M. & Barker, E. (2008). A New Bond Albedo for Performing Orbital Debris Brightness to Size Transformations. *2008 International Astronautical Congress*, Glasgow, Scotland, October 2008.
28. Mulrooney, M., Matney, M.J., Hejduk, M.D. & Barker, E. (2008). An Investigation of Global Albedo Values. In *Proceedings of Advanced Maui Optical and Space Surveillance Technologies Conference*, September 2008.
29. Hall, D. (2010). Surface Material Characterization from Multi-Band Optical Observations. In *Advanced Maui Optical and Space Surveillance Technologies Conference*, September 2010.
30. Cao, Y., Wu, Z., Bai, L. & Zhang, H. (2010). Measurement of Optical Characteristics of Solar Panels Used on Satellites. In *Proceedings of the 9th International Symposium on Antennas, Propagation and EM Theory*, IEEE, pp. 746-748.
31. Hall, D. & Kervin, P. (2014). Optical Characterization of Deep-Space Object Rotation States. In *2014 AMOS Conference*, Maui, HI, September 2014, pp. 9-12.

32. Han, Y., Sun, H., Feng, J., & Li, L. (2014). Analysis of the optical scattering characteristics of different types of space targets. *Measurement Science and Technology*, 25(7), 075203.
33. Bédard, D., & Lévesque, M. (2014). Analysis of the CanX-1 Engineering Model Spectral Reflectance Measurements. *Journal of Spacecraft and Rockets*, 51(5), 1492-1504.
34. Cowardin, H.M., Hostetler, J.M., Murray, J.I., Reyes, J.A., & Cruz, C.L. (2021). Optical Characterization of DebrisSat Fragments in Support of Orbital Debris Environmental Models. *The Journal of the Astronautical Sciences*, 68, 1186-1205.